Thermodynamics of Materials

22th Lecture

2008. 6. 4 (Wednesday)

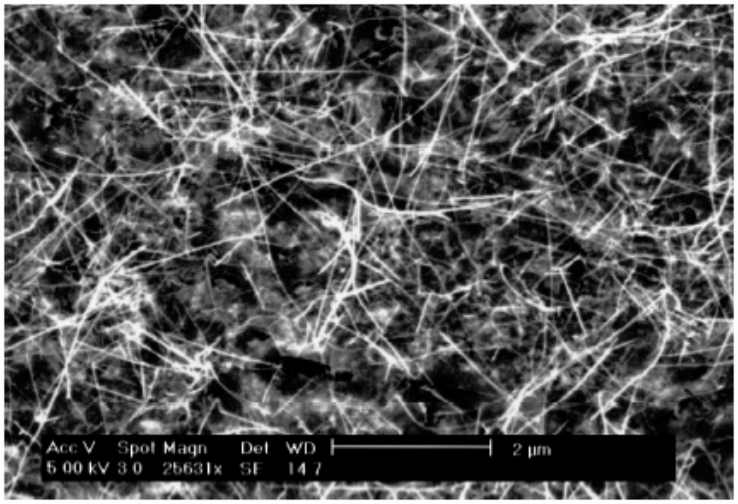

Fig. 2. SEM image of the GaN nanowires on the substrate.

H.Y. Peng et al. / Chemical Physics Letters 327 (2000) 263–270

Spontaneous Polarization-Induced Nanohelixes, Nanosprings, and Nanorings of Piezoelectric Nanobelts

Xiang Yang Kong and Zhong Lin Wang*

NANO LETTERS

2003
Vol. 3, No. 12
1625−1631

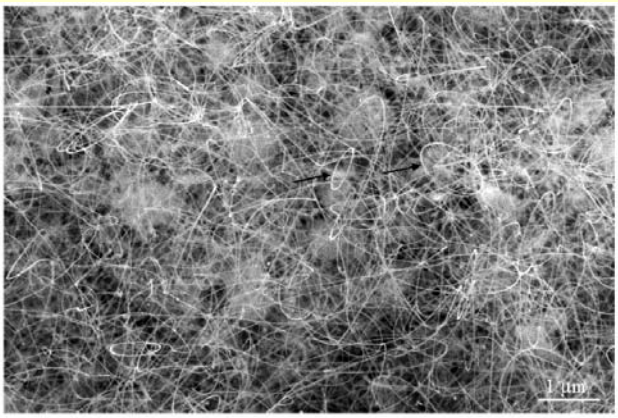

Figure 1. SEM images of the as-synthesized ZnO nanobelts, showing nanobelts of sizes 20−60 nm in widths and a large fraction of nanorings and helical nanostructures.

J|A|C|S
ARTICLES
Published on Web 00/00/0000

Formation of Piezoelectric Single-Crystal Nanorings and Nanobows

William L. Hughes and Zhong L. Wang*

Contribution from the School of Materials Science and Engineering and School of Chemistry and Biochemistry, Georgia Institute of Technology, Atlanta, Georgia 30332-0245

Received February 10, 2004; E-mail: zhong.wang@mse.gatech.edu

Abstract: Bending of polar-surface-dominated (PSD) nanobelts of ZnO can be explained by one of two processes: electrostatic neutralization of the dipole moment via deformation (called an electrostatic polar charge model) or imbalances between surface tensions via surface-termination induced stresses. This article presents experimental data on the structural features of *nanorings* and *nanobows* formed by bending single-crystal, PSD ZnO nanobelts. Our data exclusively support the electrostatic polar charge model as the dominant mechanism for bending.

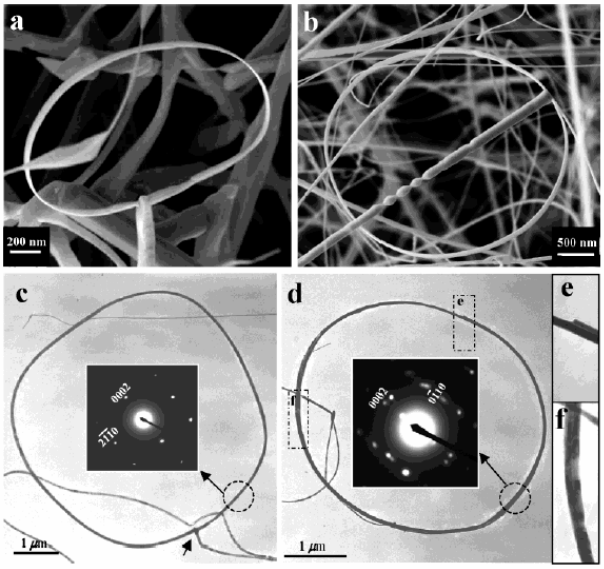

Figure 1. ZnO nanorings made from individual polar surface-dominated single-crystal nanobelts. (a,b) SEM images showing the geometry of various types of nanorings. (c,d) TEM images and the corresponding electron diffraction patterns showing the geometry and crystallographic structure of nanorings. (e) TEM image showing overlap between successive loops of a Zn- and O-terminated surfaces. Physical contact occurs between the polar surfaces of opposite charge. (f) TEM image showing the uniform strain found within a nanoring.

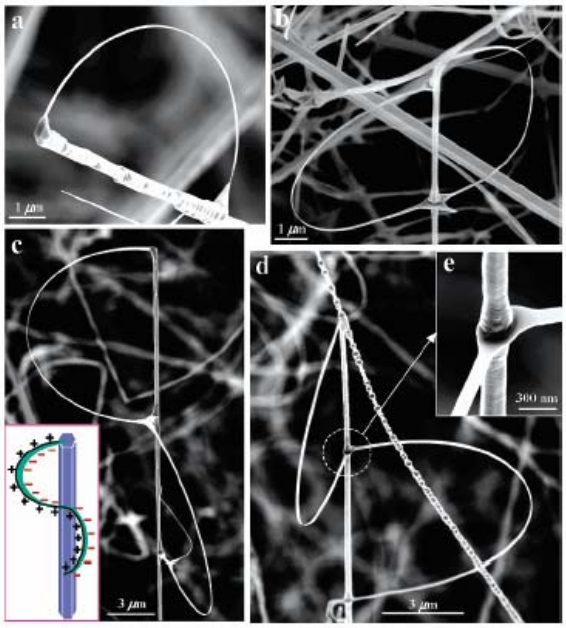

Figure 3. ZnO nanobows made from individual polar surface-dominated single-crystal nanobelts. A collection of typical geometrical shapes of the nanobows are presented. A model for the nanobow shown in (c) is inserted, showing their geometry and charge distribution along their polar surfaces (see text for details).

Ultrawide ZnO nanosheets

Jae-Hwan Park,* Heon-Jin Choi, Young-Jin Choi, Seong-Hyung Sohn and Jae-Gwan Park KIST

J. Mater. Chem., 2004, **14**, 35–36

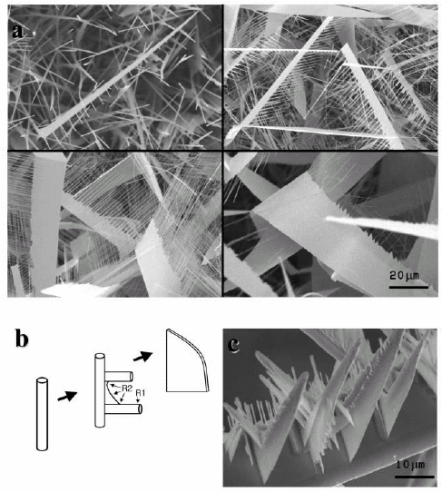

Fig. 3 (a) SEM images showing the evolutionary stages of the nanosheets from the comb-like structure toward the sheet structure, which were obtained by controlling the growth time from a few seconds to several hours. (b) A schematic illustration showing the possible growth mechanism of the ultrawide nanosheets. (c) Hierarchical 3D arrays of nanosheets.

In-situ Measurements of CNPs by nano-DMA

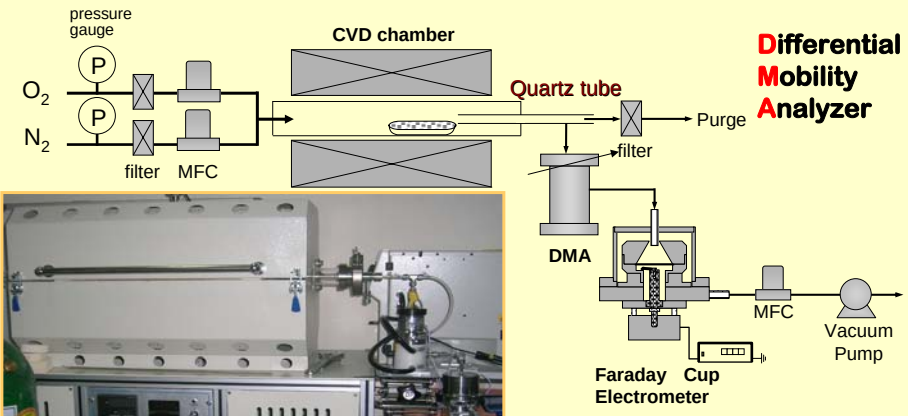

Differential Mobility Analyzer

Atmospheric CVD

1. ZnO Nanowires
2. Carbon Nanotubes
3. Si CVD

Schematic diagram of DMA

DMA can be used to produce aerosols of known size concentration and composition.

Charged particles are electrically classified by differences in their electrical mobility.

$$Z_{pc} = \frac{Q_c \ln(R_1/R_2)}{2\pi LV}$$

$$D_p = \frac{peC_c}{3\pi\eta Zp}$$

Z_{pc}= electrical mobility
Q_c= flow rate of sheath gas
D_p= particle diameter
p= number of elementary charge units
e= elementary unit of charge (1.6×10^{-19} C)
Cc= Cunningham correction factor
h= gas viscosity

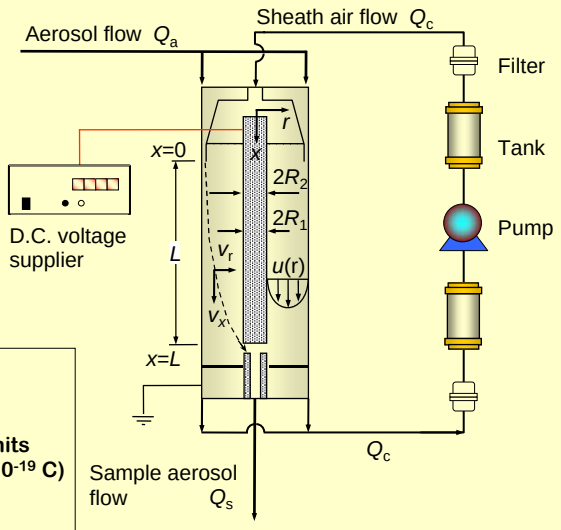

CNC, FCE, PSM

Schematic diagram of Faraday Cup Electrometer (FCE)

For particles in the 1~20nm, Number of elementary charge units is assumed equal to 1

Particle number concentration can be calculated by the following equation:

$$N = I/q_e e$$

N=particle number concentration [#/cc]
I=electrometer current [A]
q_e=aerosol flow rate [cc/s]
e=1.6×10^{-19} [C]

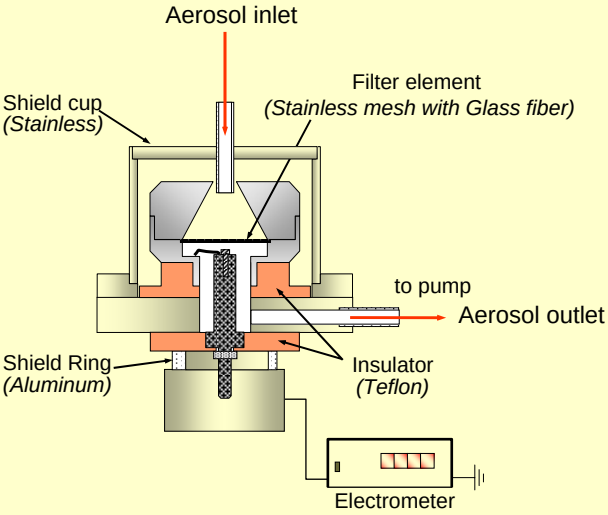

detection limits is 10^{-16} A

1) Size Distribution of Charged Nanoparticles measured by nano-DMA during synthesis of ZnO Nanowires

(a) Positive **(b) Negative**

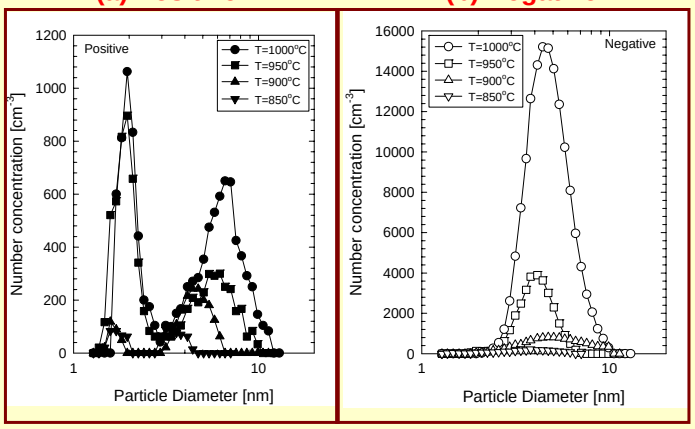

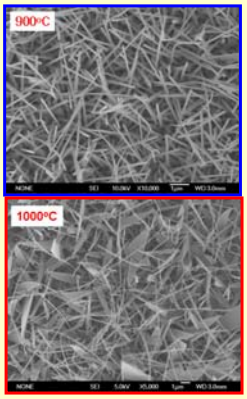

Number density increases with increasing temperature.

N_2=1.0 l/min
O_2=10ccm
ZnO:C=2:2

Particle Size Distribution of ZnO without Au-Si Substrate

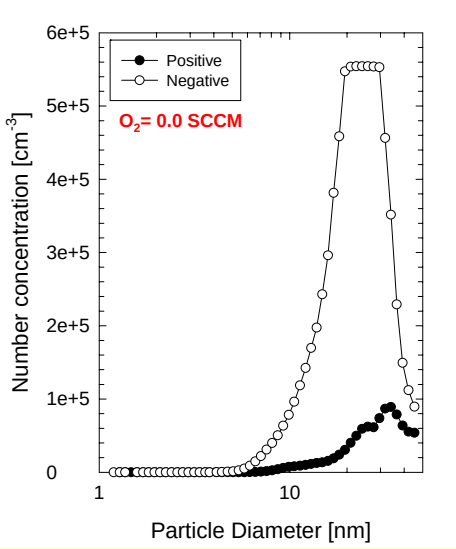

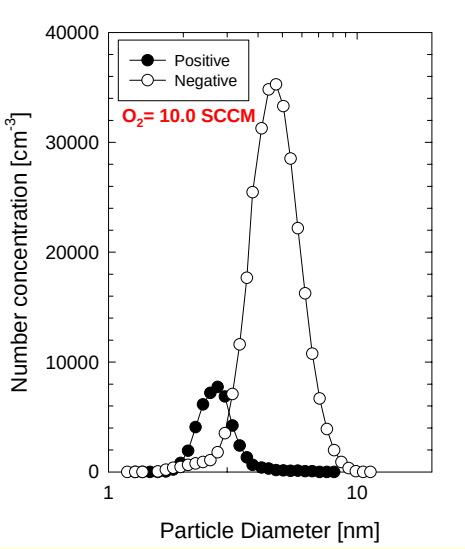

Furnace temperature=1000°C, N_2= 1.0 l/min, with Precursor (ZnO+graphite)

Effect of oxygen concentration on mophology

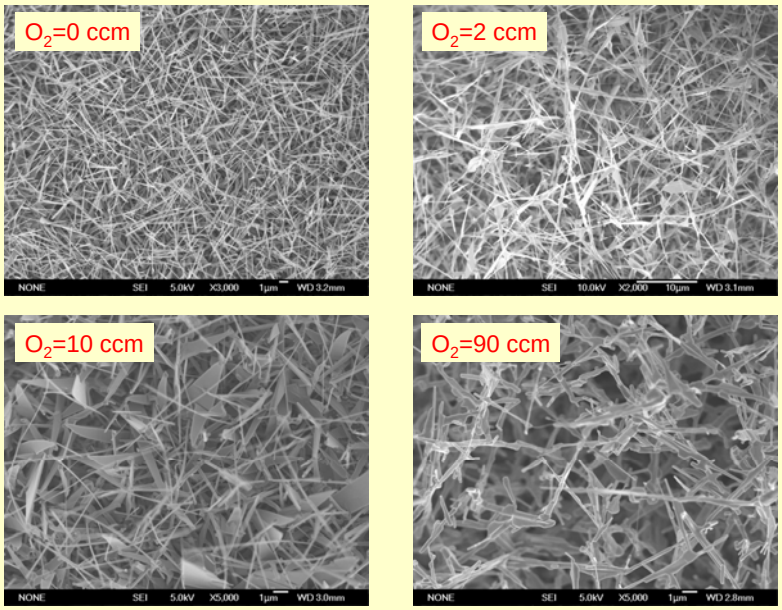

ZnO:C=2:2, T=1000°C

TEM Images of ZnO

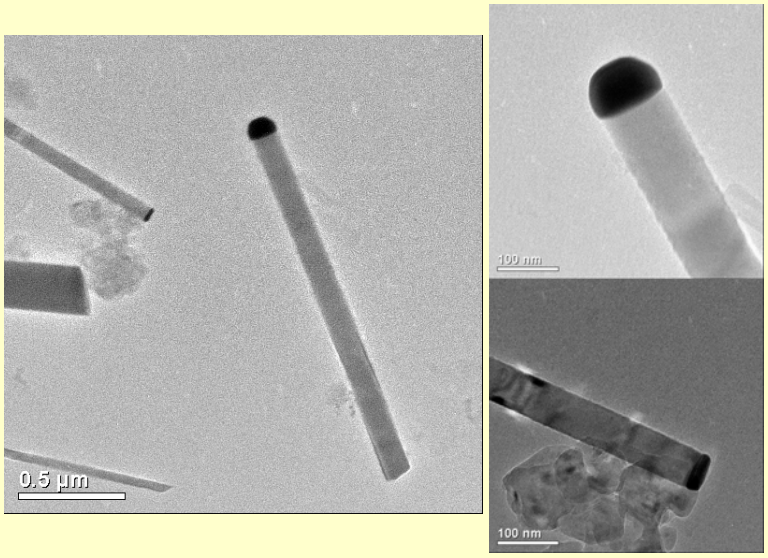

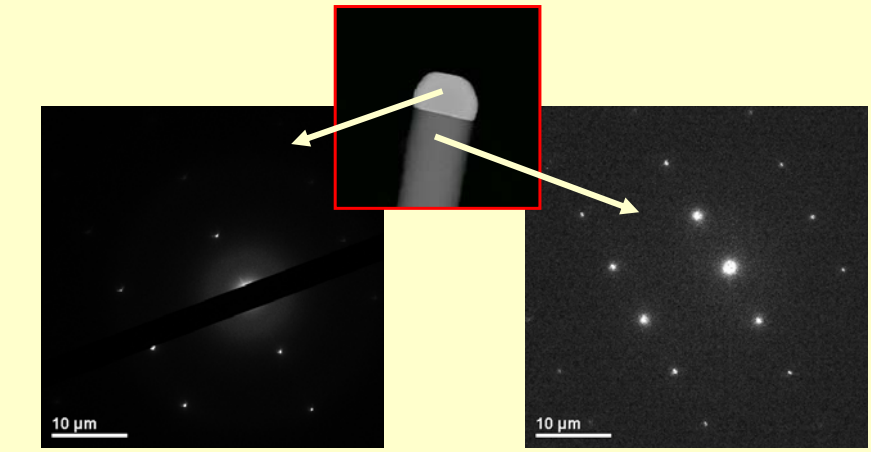

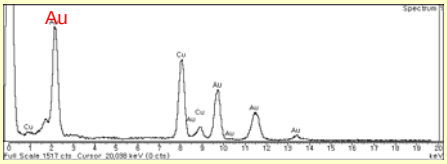

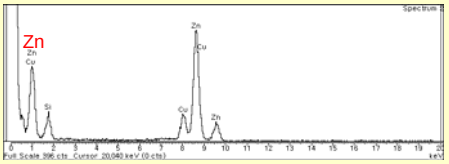

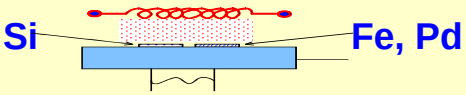

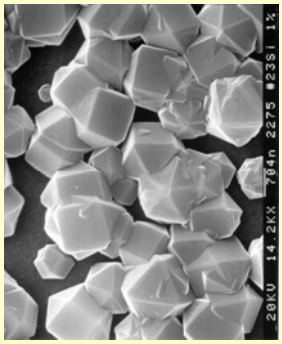

Diamond on Si

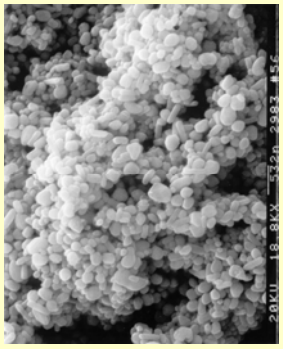

Soot on Fe

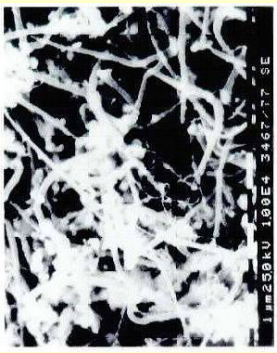

CNTs on Pd

Growth mechanisms of diamond, soot and CNTs are related to each other.

Growth of Carbon Nanotubes in the Diamond CVD Process

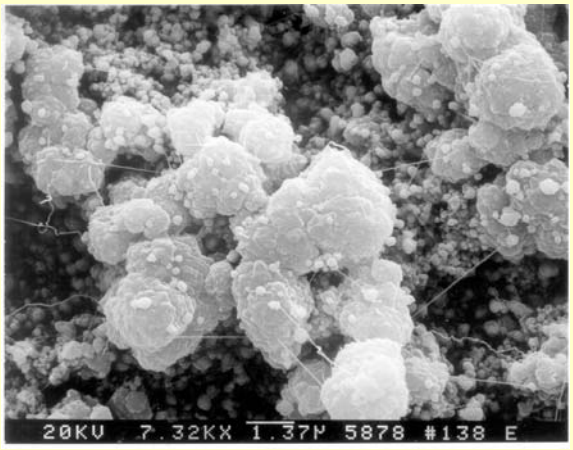

2%CH_4-98%H_2, 20 torr, 8 mm, 2 h

Possibility of Charged Nanoparticle Generation during Synthesis of Carbon Nanotubes

Generation of charged nanoparticles is experimentally confirmed in the diamond CVD process.
→ 1 ~ 5% CH_4, 95 ~ 99% H_2

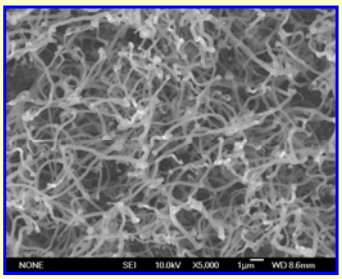

Much high concentration of CH4 is used in CNT process.
→ 20% CH_4, 80% H_2 + Catalyst

Higher CH_4 concentration in CNT process
→ higher Supersaturation
→ higher chance of gas phase nucleation

3 Electrostatic precipitators have been utilized in the beginning of last century for removing suspended dusts in flue gas, and have been widely used to protect environment. At first I would like to explain the principle of electrostatic precipitation. Corona discharge is used to generate mono-polar ionic field. Ions are driven by the electric field and charge the suspended particles[1,2].

3

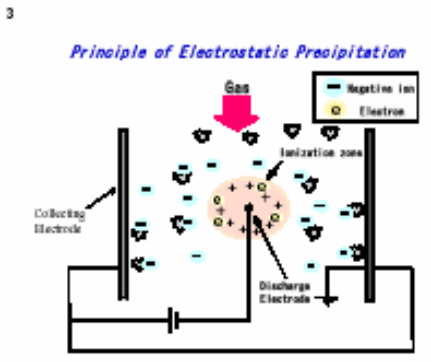

20 Those are filters after sampling the exhaust. With the voltage on, gas becomes cleaner at the center.
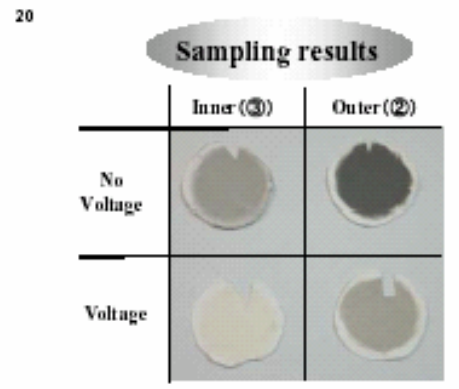
20